Published in final edited form as:
J Orthop Res. 2012 June ; 30(6): 965–972. doi:10.1002/jor.22012.

Structural and Mechanical Effects of In Vivo Fatigue Damage Induction on Murine Tendon

Jedd B. Sereysky, **Nelly Andarawis-Puri**, **Karl J. Jepsen**, and **Evan L. Flatow**
Leni and Peter W. May Department of Orthopaedics, Mount Sinai School of Medicine, New York, New York 10029

Abstract

The purpose of this study was to develop and validate an in vivo mouse model of tendon fatigue and use this model to investigate and quantify the physical manifestations of fatigue damage in mouse tendon. Patellar tendons of C57BL/6J mice were fatigue loaded at 2 Hz to three endpoints (4 N peak force per cycle for 1 h, 6 N for 1 h, and 4 N for 2 h), during which hysteresis, tangent stiffness, and peak strain of each cycle were measured. Damage accumulation was then quantified using in situ histology, and each tendon was loaded monotonically to failure. Histological damage increased significantly in all three groups (≥2-fold), and monotonic stiffness decreased significantly in the 6 N, 1 h and 4 N, 2-h groups (~25%), suggesting that damage initially manifests as changes to the collagen structure of the tendon and subsequently as changes to the function. For the fatigue loading protocols used in this study, none of the evaluated real-time parameters from fatigue loading correlated with damage area fraction measured structural damage or monotonic stiffness, suggesting that they are not suited to serve as proxies for damage accumulation. In future studies, this model will be used to compare the biological response of mouse tendon to fatigue damage across genetic strains.

Keywords

tendon; collagen; damage; microstructure; murine

Based on clinical observations, tendon failure is widely attributed to the cumulative process of overuse.[1] To study this, several sub-rupture tendon fatigue/overuse animal models have been developed,[2–5] which have revealed the effect of the pathology on tendon structure and function. Despite the insights gained from these models, a thorough understanding of the underlying molecular mechanisms has remained elusive.

Given the abundance of well-characterized inbred genetic strains of mice as well as the established technology for knocking out specific genes, the mouse model provides an advantage for studying the biological response to tendon fatigue. While a mouse model does exist in the literature,[5] the mechanism of damage induction (treadmill running) has the potential to introduce confounding factors when attempting to compare biological responses among genetic strains, due to differences in gait from animal to animal and differences in rate of damage accumulation between strains. To minimize such confounding factors it is important to ensure that similar levels of fatigue damage have been instilled despite natural variation in structural and mechanical properties of tendon among inbred strains.[6] However,

Correspondence to: Evan L. Flatow (T: 212-241-1663; F: 212-427-0208 evan.flatow@mountsinai.org).

Additional supporting information may be found in the online version of this article.

before comparing multiple strains of mice, the physical manifestations of fatigue damage for a single strain must be known.

To that end, our goal was to develop and validate an in vivo, sub-rupture tendon fatigue model in the mouse with precise input parameters and quantifiable measures of damage accumulation. Using this model, we hypothesized that: (i) mechanical parameters measured during fatigue loading can serve as proxies for damage accumulation; specifically that hysteresis would decrease, tangent stiffness would increase, and peak strain of each fatigue cycle would increase in a predictable manner as a function of damage accumulation, and (ii) damage accumulation will result in quantifiable changes to tendon structure and function; specifically an increase in histological damage area fraction (DAF) and a decrease in stiffness during monotonic load-to-failure tension tests. Identifying appropriate and readily obtainable measures of fatigue damage accumulation in this model will allow future studies to compare and contrast the biological response to the same amount of damage induction across genetically distinct strains.

MATERIALS AND METHODS

Adult (16- to 52-week-old) female C57BL/6J mice (18.39–28.77 g) (The Jackson Laboratory, Bar Harbor, ME) were used and randomly assigned to all groups. All procedures were approved by the Institutional Animal Care and Use Committee.

Patellar Tendon Mechanical Properties

To assess patellar tendon mechanical properties, hind limbs from four mice were harvested and the skin and fascia surrounding each patellar tendon was removed. For each limb (n = 8), the patella was gripped between its medial and lateral aspects using a custom clamp, the tibia was gripped proximally using modified forceps. The placement of the clamps ensures that the patellar tendon is mechanically isolated, and that sub-patellar connective tissues are not stretched. The patellar clamp was connected in series with a 10 lb load cell to an Instron (Instron, Norwood, MA) (Fig. 1), and the tibial clamp was secured to the test platform using a base consisting of an adjustable vise (PanaVise Products, Inc., Reno, NV) and an X–Y translation stage, allowing the tendon to be aligned with the loading axis. The tendon was then preconditioned by cyclical loading from 0.5 to 1.5 N, at a rate of 2 Hz, correlating to a physiologic loading rate, for 10 cycles, and monotonically loaded from 0.5 to 4.0 N at 0.5% strain/s, allowed to recover for 10 min, and subsequently monotonically loaded to failure at 0.5% strain/s. Repeated loading was performed to ensure that the strain rate selected yielded reproducible results by comparing sequentially recorded stiffness values. An additional eight hind limbs were similarly prepared, preconditioned, and monotonically loaded to failure at 0.5% strain/s, to record monotonic stiffness and failure load. Load and displacement data were collected for these and all mechanical tests at 100 Hz. A line was fit to 200 data points (2 s) in the linear region of the load-displacement curve, allowing inclusion of the majority of the linear portion of the curve while excluding all other portions of the curve. The slope of the best fit line was recorded as the stiffness of the tendon. The peak force measured was recorded as the failure load.

Strain Measurement Validation

In order to confirm that applied loads directly translated into tendon loading, six patellar tendons were prepared for mechanical testing and stain lines were applied to the surface of the tendon at the extremes using graphite powder (Asbury Carbons, DeQuincy, LA). The tendons were preconditioned as previously described, and loaded monotonically to failure at 0.5% strain/s. Surface strain data were acquired videographically using a camera at 10 Hz (Fig. 1b).

Sequential frames were imported into image processing software (IMAQ Image Builder, National Instruments, Inc., Austin, TX) which was used to automatically identify the stain lines and clamp positions in each frame. The distances between the centroids of the stain lines as well as the positions of the edges of the clamps were then calculated, from which surface and clamp strains were calculated for each frame. Strain was calculated again using the recorded position of the actuator when each frame was captured,

$$\mathrm{Strain}_{\mathrm{Surface}}=\frac{L_f-L_0}{L_0} \quad \mathrm{Strain}_{\mathrm{Clamps}}=\frac{X_f-X_0}{L_0}$$
$$\mathrm{Strain}_{\mathrm{Actuator}}=\frac{D_f-D_0}{L_0}$$

where L_f is the length of the tendon in each frame, L_0 is the initial length of the tendon, X_f is the length between the clamps in each frame, X_0 is the initial distance between the clamps, as measured videographically, and D_f is the length between the clamps in each frame and D_0 is the initial distance between the clamps, as measured by the actuator.

In Vivo Accumulation of Fatigue Damage

Eighteen mice were continuously administered gas (isoflurane) anesthesia (2% by volume, 0.3 L/min). Once surgical anesthesia was attained, each animal was secured, supine, on a Plexiglas frame (Fig. 1a). The frame was attached to an adjustable vise to facilitate positioning of the animal and maintaining a physiologic knee flexion angle of ~30° during the loading tests. A 1 cm longitudinal incision was made to expose the tibia, patellar tendon, and patella. The tibia and patella were gripped and the tendon was positioned and preconditioned in the same manner as previously described for isolated limbs. The tendon was then cyclically loaded in tension at 2 Hz, between 0.5 N and 4.0 N. Six mice were fatigued for 1 h (4 N, 1-h group) and six mice were fatigued for 2 h (4 N, 2-h group). Six additional mice were loaded between 0.5 N and 6.0 N for 1 h (6 N, 1-h group). Loading conditions were varied to determine if the amount of damage instilled could be modulated by altering the fatigue input parameters. Load-deformation data were acquired at 100 Hz continuously throughout the fatigue life, and was used to measure hysteresis, tangent stiffness (using the linear portion of the loading curve), and peak strain for each cycle. Change in hysteresis, tangent stiffness, and peak strain were calculated using the fatigue loading data by comparing the averaged values for the initial and final 100 cycles. Twelve mice underwent sham surgery ($n = 6$ for 1 h and $n = 6$ for 2 h). The sham surgery was identical to the fatigue loading surgery, with the exception that the patellar tendon remained under no force throughout the duration of the experiment. All mice were killed immediately after surgery and the hind limbs underwent SHG imaging followed by monotonic testing. To confirm the feasibility of our model for survival studies, an additional six mice were fatigued between 0.5 N and 4.0 N for 2 h, after which the grips were removed, incisions were sutured (Proline, Ethicon, Somerville, NJ), analgesia (Buprenorphine, 0.2 mg/kg) was administered subcutaneously and the mice were returned to their cages.

In Situ Imaging

To capture physical measures of damage nondestructively (allowing subsequent mechanical testing on the same sample), second harmonic generation (SHG) imaging was performed on each exposed, unfixed, unstained tendon (both fatigue/sham and contralateral) in situ with the limb maintained in a physiologic flexion angle of ~30°, to reveal collagen architecture. Imaging was done immediately after each mouse completed fatigue or sham loading. An upright laser-scanning multiphoton microscope (BioRad Radiance2000; Carl Zeiss Microimaging Inc., Thornwood, NY), with a 10-W Verdi V10-Mira 900 Ti:Sapphire laser (Coherent Inc., Santa Clara, CA) tuned to 840 nm was used, with a 60× (NA = 0.9) water

immersion objective. Reflected SHG signals were collected using an external detector via a bandpass filter (450/80 nm). Under these configurations, 8-bit grayscale images were acquired with 1,024 × 1,024 pixel resolution on a field of view of 205 μm at 1 μm optical sections through the entire thickness of the midsection of the tendon, in accordance with or previously published protocol.[7]

SHG Image Analysis

SHG images were analyzed in accordance with our previously published protocol.[7] Images (n = 60, 1 image per tendon) were analyzed manually to provide a gold standard for optimizing the damage quantification algorithm. A grid was superimposed on each image and each box within the grid was determined to be damaged or not damaged by a trained, blinded user. A box was determined to be damaged if it contained any collagen fibrils that were distorted, relative to the collagen fibril orientation of adjacent boxes. The number of damaged boxes normalized by the total number of boxes yielded the DAF of each image.

All images were subsequently analyzed automatically. Each image was sub-divided into 400 (20 × 20) boxes (similarly to the manual method) and each box (51 × 51 pixels; 7.2 × 7.2 μm^2) was converted into its fast Fourier transform power spectrum (FFT-ps). An ellipse was then fit to the highest intensity region of the FFT-ps. Given the nature of the FFT-ps, the orientation of the collagen within the box is parallel to the minor axis of the ellipse. The collagen orientation of each box was then compared to those of adjacent boxes to determine if the box of interest was damaged, using the same criteria as was used for manual analysis. Specifically, boxes were determined to be damaged if the measured collagen fibril orientation differed from that of adjacent boxes by more than a preset threshold (4°). The box size and preset threshold were identified by iteratively adjusting each value until the results of the automatic DAF analysis most closely correlated with the results of the manual analysis, as previously published.[1] Again, the number of damaged boxes was normalized by the total number of boxes to yield the DAF of each image. Damage is manifested as kinks in the ECM collagen, abrupt changes in the collagen fibril orientation that remain when the tendon is under physiologic tension (as was done for all SHG images collected), and thus can be rigorously defined as a change in collagen fibril orientation (measured in degrees) between two regions of interest greater than a defined threshold. Alternately adjusting the algorithm's two inputs, box size and threshold for angle differences above which the box of interest would be considered damaged, the automatic method was optimized to yield DAFs that correlated best with those of the manual analysis.

Monotonic Testing

To determine the effect of fatigue damage on monotonic stiffness and failure load, each patellar tendon (both fatigue/sham and contralateral) was monotonically loaded to failure immediately after imaging, as previously described.

Statistical Analysis

All data are reported as mean ± SD, and $p \leq 0.05$ represents statistical significance for all statistical tests. All multiple group comparisons were made using one way ANOVA with post hoc Bonferroni, and all two group comparisons were made using a paired, two-tailed t-test.

RESULTS

Patellar Tendon Mechanical Properties

No differences in elastic moduli among repeated force-deformation curves confirmed that loading specimens at 0.5% strain/s yields reproducible results (p = 0.78). The monotonic

stiffness was 49.62 ± 10.82 N/mm and the tensile strength was 9.15 ± 1.93 N. The mid-toe region was determined to be 0.5 N and was used as the lower bound for preconditioning and fatigue loading. 4 N and 6 N corresponded to the mid-physiologic region (~45% and ~65% of the monotonic failure load, respectively) and were used as the upper bound of fatigue loading.

Determination of Measured Strain Fidelity

Surface strain and actuator strain correlated well, yielding an R^2 of 0.61 ± 0.41; however, the average slope of the best fit lines was 1.50 ± 0.80, indicating that there is compliance in the testing system. Surface strain and clamp strain correlated well, yielding an R^2 of 0.74 ± 0.18, with an average best fit slope of 1.01 ± 0.55 ($p < 0.0001$ for all correlations), confirming that the clamps do not slip. All displacement measurements were then made using the recorded actuator displacement, corrected using the slope of the average best fit line of the surface strain-actuator correlations to account for this compliance.

In Vivo Loading

Changes in hysteresis, tangent stiffness, and strain were determined from the fatigue data (Fig. 2), and are reported in Table 1. Hysteresis changes, stiffness changes, and peak strains did significantly change during fatigue loading ($p < 0.02$ for all groups), however, the changes were not significantly different between the three-loaded groups ($p = 0.69$, $p = 0.54$, $p = 0.07$, respectively), although peak strain exhibited a trend. To investigate this, peak strain curves were then fit using bilinear regression, fitting the first line to the primary phase and the second line to the secondary phase ($R^2 = 0.77 \pm 0.20$). The slope of the primary phase and secondary phase and the cycle number of the junction between the two were not significantly different between the three groups ($p = 0.15$, $p = 0.87$, $p = 0.14$, respectively). Pooling the data from the three groups, the slope of the primary phase was $3.44 \times 10^{-3} \pm 5.61 \times 10^{-3}$ and the slope of the secondary phase was $2.26 \times 10^{-5} \pm 6.32 \times 10^{-5}$. None of the parameters (changes in hysteresis, tangent stiffness, and peak strain, the slopes of the primary and secondary phase of peak strain over time) correlated significantly with monotonic stiffness ($p = 0.84$, $p = 0.66$, $p = 0.31$, $p = 0.48$, $p = 0.90$, respectively) or DAF ($p = 0.16$, $p = 0.74$, $p = 0.54$, $p = 0.91$, $p = 0.66$, respectively). All survival mice awoke and ambulated normally (no visible limping) within 20 min of cessation of anesthesia confirming that our in vivo fatigue accumulation model is well tolerated by the animals. Survival mice were kept alive for up to 8 weeks post-fatigue (at which point they were killed for another study). When examined, all survival mice exhibited healing of their surgical wounds without complication.

Monotonic Testing

Failure load and monotonic stiffness were determined using the monotonic loading data. No significant differences in failure load were observed (Fig. 3a). Monotonic stiffness loss of 28.62% was observed in 6 N, 1 h, relative to its contralateral control ($p = 0.03$) and a loss of 31.25% was observed in 4 N, 2 h, relative to its contralateral control ($p = 0.05$) (Fig. 3b). Monotonic stiffness did not correlate with age ($R^2 = 0.06$, $p = 0.21$).

In Situ Imaging and Analysis

SHG images of physiologically positioned, unstained, unfixed tendon in situ revealed collagen orientation clearly (Fig. 4). DAF values for images analyzed manually and automatically correlated well ($R^2 = 0.63$) and were significant ($p < 0.0001$) (Fig. 5). DAF increased 2.8-fold for 4 N, 1 h, relative to contralateral control ($p = 0.03$), 2.0-fold for 6 N, 1 h, relative to contralateral control ($p = 0.05$), and 3.0-fold for 4 N, 2 h relative to contralateral control ($p = 0.03$). DAF values did not correlate with age ($R^2 = 0.05$, $p = 0.36$).

No differences were observed between sham-operated tendons and their contralateral controls, confirming the ability of the algorithm to capture the baseline state of the tendon (Fig. 6).

DISCUSSION

Our studies have demonstrated the feasibility of mechanically loading mouse patellar tendons in vivo and subsequently monotonically testing them, allowing us to identify the mechanical properties of patellar tendons of the C57BL/6 mouse, a commonly studied genetic background, and investigate overuse tendinosis in vivo. The age range used in this study was chosen to include animals that are sexually and skeletally mature, but not elderly.[8] No significant correlations were observed between age and either DAF or stiffness within contralateral, healthy limbs, suggesting that age, within this range of adulthood, does not affect structure or function.

We have demonstrated that clamp strain correlates well with surface strain, confirming that our gripping technique is suitable for mechanical testing and ensuring that our control over the fatigue input parameters is precise. Additionally, the rapid recovery of the survival cohort confirms that this surgical regimen is suitable for performing survival studies. Furthermore, SHG imaging of the unstained, unfixed tendon in situ revealed that collagen fibril orientation was clearly visible, suggesting that in future studies, SHG imaging could be performed in vivo, on anesthetized mice, allowing damage accumulation (or structural changes subsequent to damage induction) to be measured in the same animal repeatedly during the survival period. Furthermore, the SHG images of mouse tendon revealed collagen architecture and damage manifestation similar to that of rat (Fig. 4).[2,7,9] These similarities include the presence of periodic crimp present in lax tendon which are minimized with physiologic tension, and the presence of kinks subsequent to damage accumulation, which remain under physiologic tension. These similarities allowed our automated DAF algorithm, which was developed in rat, to be easily optimized for use in mice.

Variation was observed in the DAF values and monotonic stiffness of contralateral, healthy limbs. The presence of structural damage in “healthy” tendon has also been observed in human[1] and rat tendon.[10] This natural variation of parameters measured makes it advantageous to use each animal as its own control, which was achieved by the use of paired *t*-tests, comparing each loaded limb to its contralateral.

Our initial cohort of in vivo, fatigue-loaded mice (4 N, 1 h) did not exhibit a measurable accumulation of fatigue damage, as measured by monotonic stiffness loss relative to contralateral, but did exhibit an increase in DAF, demonstrating that structural changes are present in the tendon prior to measurable changes in monotonic stiffness. We subsequently increased the amount of fatigue damage accumulation in two ways: by increasing the peak force of each cycle (6 N, 1-h group) and by increasing the number of cycles for fatigue loading (4 N, 2-h group). Increasing either the peak force or increasing the number of cycles maintained a significant increase in DAF of ≥2-fold, and additionally yielded significant decreases in monotonic stiffness of ~30%. The presence of monotonic stiffness loss in 6 N, 1 h and 4 N, 2 h observed with a small sample size, indicated additional fatigue damage accumulation beyond that of 4 N, 1 h (for which no stiffness loss was observed), demonstrating our model’s strength of allowing the investigator to perturb one of several of the fatigue input parameters to control the level of fatigue damage instilled. Neither of the sham surgery control groups had a significant increase in DAF or loss of monotonic stiffness relative to their contralateral limbs, indicating that the DAF increases and stiffness losses observed were due to fatigue loading and not the surgical procedure.

Interestingly, despite the indication of additional fatigue damage accumulation in 6 N, 1 h and 4 N, 2 h, the DAF did not increase in those groups. One potential explanation is that, in mice, DAF increases significantly initially (4 N, 1 h), but that additional damage, as was accumulated in 6 N, 1 h and 4 N, 2 h, does not increase the DAF but rather increases the amount of damage within previously damaged regions. Another consideration is that by using SHG, we have only examined potential changes to the collagen structure. Molecular studies, such as in situ hybridization or immunohistochemistry investigating ECM components excluding type I collagen fibrils, such as type XII collagen or proteoglycans, may reveal fatigue-damage dependent changes that take place. These studies may be particularly relevant given that these matrix components are known to have an effect on function.[11] Future studies will investigate the manifestation of damage at various points in the fatigue life of murine tendon to determine if and how histological quantification of damage accumulation can be further improved.

Our findings suggest that damage initially leads to changes in structure (as measured by DAF), and subsequently to changes in function (as measured by monotonic stiffness loss), which has led us to reject our second hypothesis—that damage accumulation will result in an increase in DAF and a decrease in monotonic stiffness. We found that DAF is an early indicator of fatigue damage accumulation, and that only with additional damage accumulation does monotonic stiffness decrease. Thus, our data indicate that changes to morphology of ECM collagen are an accurate measure of early-stage fatigue damage accumulation, but that stiffness loss is a more sensitive measure of late-stage fatigue damage accumulation. Interestingly, the decrease in monotonic stiffness is not associated with further increase in DAF. This suggests that using both DAF and monotonic stiffness loss together allows a larger range of fatigue damage accumulation to be quantified than using either parameter alone.

Tendon's ability to maintain mechanical properties until accumulating a significant amount of fatigue damage is in accordance with previously published findings,[9] however, our analysis of structural damage reveals that quantifiable damage is accumulating within the tendon throughout the fatigue process and specifically prior to changes in mechanical properties. The maintenance of function despite significant changes to structure is similar to the behavior of other musculoskeletal tissue, such as bone.[12] However, the cells within bone respond to changes in structure[13] while those of tendon may not,[1] allowing tendinosis to develop. Thus, the relationship between tenocyte and extracellular matrix that may allow such significant structural changes to go unrepaired warrants further investigation.

Changes in mechanical parameters measured during fatigue loading, though significant for each loading group, were not significantly different between loading groups, despite significant differences being observed via the post hoc tests. This suggests, contrary to our first hypothesis, that none of the parameters we measured can serve as a real-time proxy for fatigue damage accumulation. Despite having an initial primary phase in which each mechanical parameter changes drastically as a function of loading cycle, all parameters level off to a linear secondary phase with little or no slope. Furthermore, comparing the 4 N, 1 h and 4 N, 2-h groups reveals that damage accumulation takes place during the second hour of fatigue loading, in addition to the first, and that during the second hour of damage accumulation, changes in mechanical parameters are subtle. This suggests that damage accumulation alone results in subtle changes, as seen in the secondary phase, while the behavior in the primary phase is due to the superimposition of non-fatigue dependant changes to the tendon. Change in peak strain showed a trend toward being significantly different between loading groups, therefore, we further investigated peak strain as a potential measure of damage accumulation by fitting the peak strain curves using bilinear regression. This analysis revealed that none of the additional parameters generated (rate of

change of peak strain in the primary or secondary phase, or the length of the primary phase) differed as a function of loading protocol, indicating that neither the entire peak strain curve nor any component of the peak strain curve could be used as a real-time measure of damage either.

Real-time mechanical parameters measured, including the additional parameters generated from the peak strain curves, did not correlate to DAF increase or monotonic stiffness loss. This has led us to reject our first hypothesis and conclude that the mechanical parameters we measured during fatigue loading (hysteresis, tangent stiffness, and final strain) are not suited to serve as proxies for damage accumulation given the fatigue regimens we used. It may be possible that for the damage groups evaluated, extremely subtle differences in the real-time parameters could be identified by vastly increasing our sample sizes. However, identifying such differences would not be useful, as the purpose of investigating real-time parameters was to identify obvious changes that could be used to assess the damage induced in a single tendon in real-time (as opposed to a subtle difference that can only be identified by comparing an impractically high number of tendons post-hoc). Future work will further explore additional real-time parameters and more disparate fatigue regimens in an attempt to reveal predictive real-time measures. In addition, Future studies will also investigate differences in mechanical parameters collected during diagnostic tests (low force cyclic loading bouts that do not induce damage themselves) before and after fatigue loading, using more varied loading regimens, and additional real-time parameters, which may yield useful measures of damage accumulation.

Despite the lack of useful real time measures of damage accumulation, we have demonstrated that damage can be quantified post hoc by measuring DAF (non-destructively) and/or monotonic stiffness (destructively), making them useful for identifying a loading regimen that induces the desired level of damage. To accomplish this, one would need to identify mid-toe region and mid-elastic region loads for each mouse strain and use those values to define the maximum and minimum load of each fatigue cycle. The number of fatigue cycles would then have to be manipulated through trial and error for each mouse strain until similar fatigue damage was induced in both strains, as defined by DAF and/or monotonic stiffness loss. Finally, the biological responses could be investigated in survival mice of each strain, which are thus known to have accumulated similar levels of fatigue damage. Alternatively, if procedure time were an important variable to control, one could set the number of fatigue cycles as an independent variable, and determine the damage as a function of maximum load per cycle, thus manipulating maximum load per cycle to instill the desired amount of fatigue damage.

A limitation of this model, as with other published models that acutely induce damage, is that the disease process we are modeling does not occur acutely, but rather over months or years. Nonetheless, the damage we induce results in tendon matrix disorganization, which, amongst other pathologic changes, has been previously observed in macroscopically healthy human tendon, and thus attributed to overuse.[1] Furthermore, Collagen degeneration has also been observed in rats subsequent to treadmill-induced overuse[14] and mechanically induced fatigue,[2,9] establishing collagen degradation as an indication of tendinopathy. Therefore, we believe that this model will be useful for investigating relevant biological responses. Furthermore, given the potential for performing mechanical tests on genetically distinct mouse strains with different tendon mechanical properties, control over the fatigue input parameters is crucial in allowing the user to ensure that any fatigue-loaded groups being compared have accumulated comparable levels of fatigue damage, despite altered innate tendon material properties.

Another limitation of this model, as it was utilized in the current study, is that the patellar tendons are mechanically tested to failure in situ, therefore, cross-sectional area and consequently stress were not measured and calculated, respectively. Nonetheless, the mice in each cohort did not differ by age, weight, or patellar tendon length or width (data not included), suggesting that force measurements were a good proxy for stress measurements. Testing the tendons in situ allows the testing conditions to very closely mimic the in vivo loading conditions; anatomical positioning is maintained and there is no risk of mechanically damaging the tendon. In the future, the mechanical testing protocol can be altered to allow dissection of the patellar tendon and measurement of the cross-sectional area prior to monotonic testing, if desired.

In conclusion, we have developed and validated an in vivo, murine model of sub-rupture tendon fatigue. Using this model we have made progress in understanding how fatigue damage is manifested within tendon. In the future, we plan to use this model to instill comparable levels of damage among genetic mouse strains and investigate the response of tendon to fatigue damage as a function of genetic background.

Supplementary Material

Refer to Web version on PubMed Central for supplementary material.

Acknowledgments

We acknowledge Donna Kochhar for her contributions. This study was supported by NIH grants GM007280 (JBS) and AR052743 (ELF). Microscopy was performed at the MSSM-Microscopy Shared-Resource-Facility, supported with funding from NIH-NCI (CA095823), NSF (DBI-9724504), and NIH (RR09145).

References

1. Kannus P, Jozsa L. Histopathological changes preceding spontaneous rupture of a tendon. A controlled study of 891 patients. J Bone Joint Surg Am. 1991; 73:1507–1525. [PubMed: 1748700]
2. Fung DT, Wang VM, Andarawis-Puri N, et al. Early response to tendon fatigue damage accumulation in a novel in vivo model. J Biomech. 2009; 43:273–279.
3. Nakama LH, King KB, Abrahamsson S, et al. Evidence of tendon microtears due to cyclical loading in an in vivo tendinopathy model. J Orthop Res. 2005; 23:1199–1205. [PubMed: 16140201]
4. Soslowsky LJ, Carpenter JE, DeBano CM, et al. Development and use of an animal model for investigations on rotator cuff disease. J Shoulder Elbow Surg. 1996; 5:383–392. [PubMed: 8933461]
5. Szczodry M, Zhang J, Lim C, et al. Treadmill running exercise results in the presence of numerous myofibroblasts in mouse patellar tendons. J Orthop Res. 2009; 27:1373–1378. [PubMed: 19350660]
6. Wang VM, Banack TM, Tsai CW, et al. Variability in tendon and knee joint biomechanics among inbred mouse strains. J Orthop Res. 2006; 24:1200–1207. [PubMed: 16705702]
7. Sereysky JB, Andarawis-Puri N, Ros SJ, et al. Automated image analysis method for quantifying damage accumulation in tendon. J Biomech. 2010; 43:2641–2644. [PubMed: 20627302]
8. Kilborn SH, Trudel G, Uhthoff H. Review of growth plate closure compared with age at sexual maturity and lifespan in laboratory animals. Contemp Top Lab Anim Sci. 2002; 41:21–26. [PubMed: 12213043]
9. Fung DT, Wang VM, Laudier DM, et al. Subrupture tendon fatigue damage. J Orthop Res. 2009; 27:264–273. [PubMed: 18683881]
10. Fung DT, Sereysky JB, Basta-Pljakic J, et al. Second harmonic generation imaging and fourier transform spectral analysis reveal damage in fatigue-loaded tendons. Ann Biomed Eng. 2010; 38:1741–1751. [PubMed: 20232150]

11. Screen HR, Shelton JC, Chhaya VH, et al. The influence of noncollagenous matrix components on the micromechanical environment of tendon fascicles. Ann Biomed Eng. 2005; 33:1090–1099. [PubMed: 16133917]

12. Pattin CA, Caler WE, Carter DR. Cyclic mechanical property degradation during fatigue loading of cortical bone. J Biomech. 1996; 29:69–79. [PubMed: 8839019]

13. Herman BC, Cardoso L, Majeska RJ, et al. Activation of bone remodeling after fatigue: Differential response to linear microcracks and diffuse damage. Bone. 2010; 47:766–772. [PubMed: 20633708]

14. Scott A, Cook JL, Hart DA, et al. Tenocyte responses to mechanical loading in vivo: A role for local insulin-like growth factor 1 signaling in early tendinosis in rats. Arthritis Rheum. 2007; 56:871–881. [PubMed: 17328060]

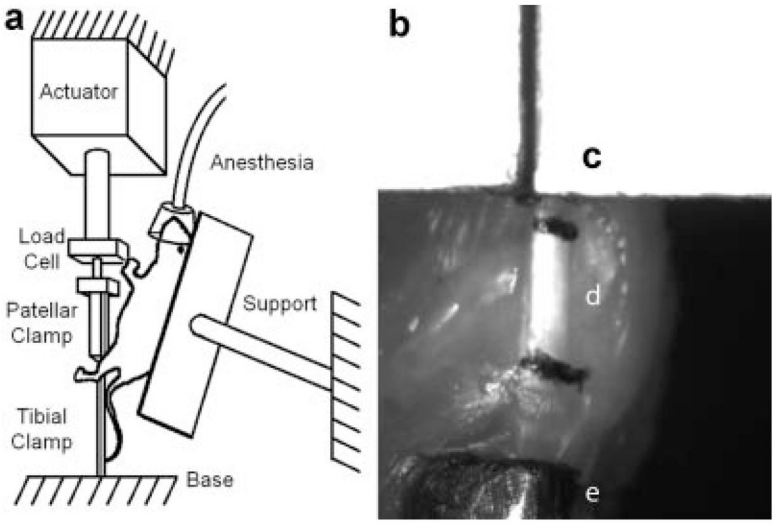

Figure 1.
Schematic of loading set-up for fatigue loading mice in vivo (a) and image of tendon being loaded (b); patellar clamp (c), patellar tendon with stain lines at extremes (d), and tibial clamp (e) can be seen. Distance between stain line centroids and distance between clamp edges was measured and compared to recorded actuator displacement for each image frame of loading videos to confirm that the clamps do not slip and relate actuator displacement to strain in tendon.

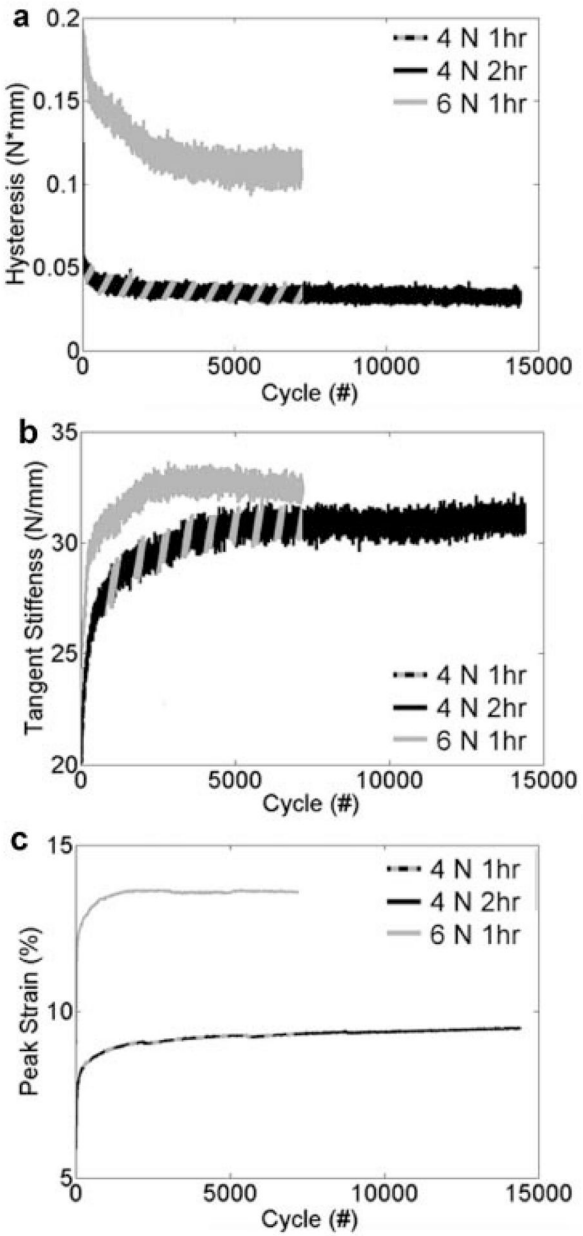

Figure 2.
Hysteresis (a), tangent stiffness (b), and peak strain (c) of each loading cycle for all three fatigue regimen.

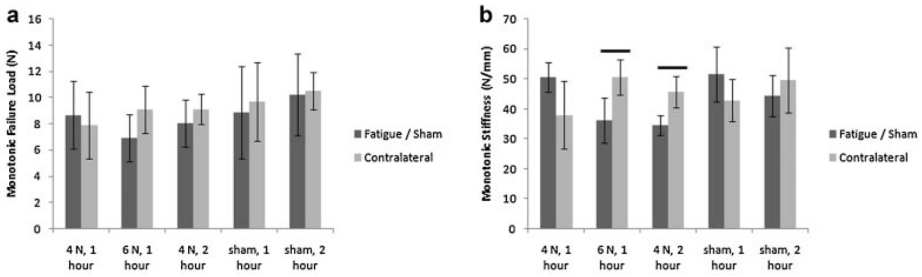

Figure 3.

Monotonic mechanical properties of fatigued and sham-operated mice. No significant differences were observed in monotonic failure loads (a), while a ~30% stiffness loss was observed in the 6 N, 1 h and 4 N, 2-h fatigue groups, relative to contralateral controls (b).

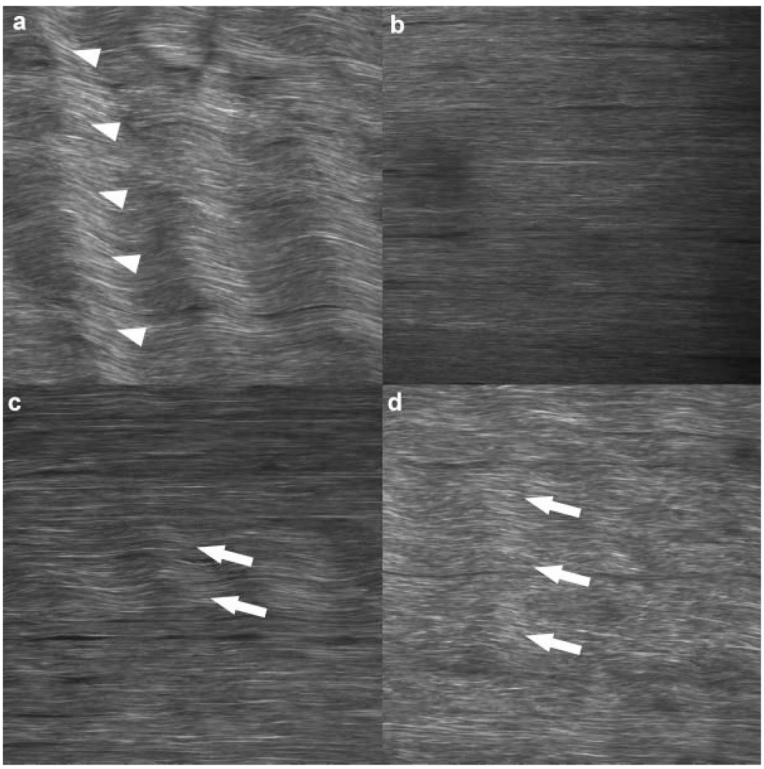

Figure 4.
Second harmonic generation image of unfixed, unstained tendon in situ, clearly revealing collagen orientation. Non-tensioned naïve tendon reveals a natural, periodic crimp (arrow heads) that runs throughout the entire width of the tissue (a), which is eliminated with physiologic positioning (b). Damage (arrows) is manifested as kinks in the collagen with defined borders during physiologic loading, which vary from smaller damage area fractions (DAF) representative of less damage (c) to higher DAFs representative of more damage (d).

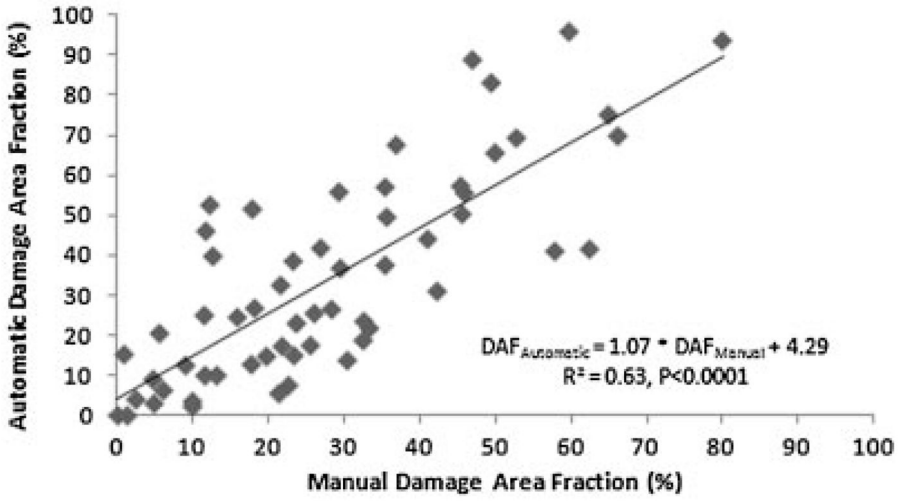

Figure 5.
Correlation of manually and automatically determined damage area fraction, a histologic measure of damage accumulation, confirming that the automated method faithfully replicates the current gold standard.

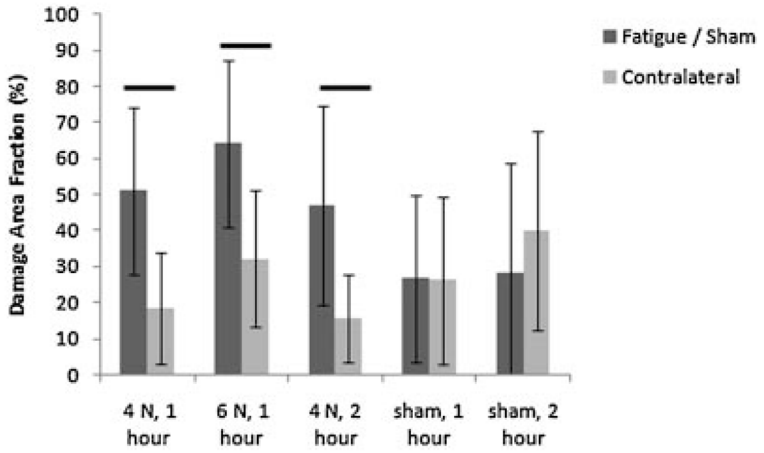

Figure 6.

Damage area fraction (DAF) of fatigued and sham-operated mice. All three fatigue-loaded groups exhibited a significant (≥2-fold) increases in DAF relative to contralateral controls.

Table 1

Percent Change in Hysteresis, Tangent Stiffness, and Peak Strain of Fatigue-Loaded Groups, Comparing the Average Value of the Initial and Final 100 Fatigue-Loading Cycles

	Δ Hysteresis (%)	Δ Tangent Stiffness (%)	D Peak Strain (%)
4 N, 1 h	−36.97 ± 16.27	24.84 ± 12.01	5.79 ± 2.57
4 N, 2 h	−32.54 ± 15.82	21.44 ± 15.47	9.42 ± 3.78
6 N, 1 h	−39.92 ± 11.44	15.51 ± 15.67	10.90 ± 7.52